Association of an Aminoacyl-tRNA Synthetase with a Putative Metabolic Protein in Archaea†

Richard S. A. Lipman,‡ Jing Chen, Caryn Evilia, Olga Vitseva, and Ya-Ming Hou*

Department of Biochemistry and Molecular Pharmacology, Thomas Jefferson University, 233 South 10th Street, BLSB 220, Philadelphia, Pennsylvania 19107

Received March 20, 2003; Revised Manuscript Received May 2, 2003

ABSTRACT: Aminoacyl-tRNA synthetases are essential enzymes that catalyze attachment of amino acids to tRNAs for decoding of genetic information. In higher eukaryotes, several synthetases associate with non-synthetase proteins to form a high-molecular mass complex that may improve the efficiency of protein synthesis. This multi-synthetase complex is not found in bacteria. Here we describe the isolation of a non-synthetase protein from the archaeon *Methanocaldococcus jannaschii* that was copurified with prolyl-tRNA synthetase (ProRS). This protein, Mj1338, also interacts with several other tRNA synthetases and has an affinity for general tRNA, suggesting the possibility of forming a multi-synthetase complex. However, unlike the non-synthetase proteins in the eukaryotic complex, the protein Mj1338 is predicted to be a metabolic protein, related to members of the family of H_2-forming N^5,N^{10}-methylene tetrahydromethanopterin (5,10-CH_2-H_4MP) dehydrogenases that are involved in the one-carbon metabolism of the archaeon. The association of Mj1338 with ProRS, and with other components of the protein synthesis machinery, thus suggests the possibility of a closer link between metabolism and decoding in archaea than in eukarya or bacteria.

Aminoacyl-tRNA synthetases (aaRSs) are essential enzymes in the pathway of decoding genetic information from DNA to RNA to protein. The 20 tRNA synthetases (one for each amino acid) are responsible for activating their cognate amino acid to generate the aminoacyl−adenylate intermediate, and catalyzing transfer of the activated intermediate to the 3′ end of the cognate tRNAs. By pairing amino acids with their cognate tRNAs, the 20 synthetases collectively establish the principle of the genetic code (*1*). On the basis of extensive structural and sequence analyses of tRNA synthetases, it is well-established that these enzymes are modular proteins made up of a conserved catalytic domain for aminoacylation, and a less conserved domain for binding of tRNA (*2*, *3*). Because of the overall similarity of the tRNA L-shaped tertiary structure, some synthetases have the ability to bind to general tRNA, which is followed by a closer discrimination for recognizing the specific tRNA (*4*). The binding of general tRNA may ultimately facilitate the overall rate of protein synthesis. Indeed, many eukaryotic synthetases differ from their bacterial counterparts by having extension and insertion domains. Some of these eukaryotic-specific domains are used to enhance general tRNA binding, such as the N-terminal extension in the yeast and rat AspRS, the N-terminal domain of the mammalian LysRS, and the C-terminal extension of human MetRS (*5*−*8*).

In higher eukarya, from flies (*Drosophila melanogaster*) to humans (*Homo sapiens*), nine synthetases (ArgRS, AspRS, GlnRS, IleRS, LeuRS, LysRS, MetRS, GluRS, and ProRS) associate with three auxiliary proteins (p18, p38, and p43) to form a stable multi-synthetase complex of ∼1000 kDa that appears to facilitate protein synthesis (*9*, *10*). The association is largely mediated by a eukaryotic-specific R domain that is present in some of the nine synthetases, such as MetRS, GluRS, and ProRS. Interestingly, GluRS and ProRS in the multi-synthetase complex are actually linked through multiple R domains to form the bifunctional Glu-ProRS (*11*). The R domain consists of imperfectly repeated units of 50−60 amino acids that have an affinity for general tRNA. This R domain is also present in the p43 auxiliary protein (*12*) and may be used to facilitate nuclear export of tRNA to the cytoplasm (*13*, *14*). The p38 protein has an affinity for several synthetases and is important for protein−protein interactions that organize the complex (*15*). The p18 protein is responsible for the transient interaction of the complex with elongation factor EF-1H (*16*). Thus, by providing multiple RNA−protein and protein−protein interactions, the complex can channel tRNA from nucleus to synthetases, to elongation factors, and to ribosomes without dissociation into the cellular matrix (*17*). This channeling network should enhance the efficiency of protein synthesis by caging tRNA in the complex, including aminoacyl-tRNA, peptidyl-tRNA, and uncharged tRNA (*18*).

The multi-synthetase complex is not visibly present in bacteria. However, little is known about synthetase organization in archaea, which consists of organisms that primarily thrive in extreme environments. While an early report presented evidence of a multi-synthetase complex in the

† Supported by NSF Grant MCB-9904956 (to Y.-M.H.), NSF Postdoctoral Fellowship DBI-0074388 (to C.E.), and American Heart Association Postdoctoral Fellowship 9920298U (to R.S.A.L.).

* To whom correspondence should be addressed. Telephone: (215) 503-4480. Fax: (215) 923-9162. E-mail: Ya-Ming.Hou@mail.tju.edu.

‡ Present address: PTC Therapeutics, 100 Corporate Court, South Plainfield, NJ 07080.

10.1021/bi0344533 CCC: $25.00
Published on Web 05/29/2003

extreme halophile *Haloarcula marismortui* (*19*), further insights from other archaeal organisms are of great interest. Because archaea account for a major portion of the global biomass and provide repositories of evolutionary information, they will shed new light on the vast biological and genetic diversity in extant life forms. Here we describe the association of ProRS in the archaeal methanogen *Methanocaldococcus jannaschii* with a non-synthetase protein that is designated Mj1338 on the basis of annotation of the genome. Mj1338 was first identified during purification of the unusual ProRS of *M. jannaschii*, whose genome lacks a recognizable gene for CysRS but encodes the activity for aminoacylation of $tRNA^{Cys}$ with cysteine (*20*). The activity was purified and shown to be encoded by a ProRS that appears to be active with both proline and cysteine (*21*, *22*). This ProRS was copurified to homogeneity with Mj1338 in similar quantities, which accounted for 0.2% of the total cellular proteins (*21*). Mj1338 is a 38 kDa protein predicted to be related to members of the family of H_2-forming N^5,N^{10}-methylene tetrahydromethanopterin (5,10-CH_2-H_4MP) dehydrogenases that catalyze an intermediate step in the C1 unit metabolism of the methanogen. The significance of Mj1338 was previously unclear, because it did not stimulate the aminoacylation activity of ProRS with proline or cysteine (*21*). However, the copurification of Mj1338 with ProRS raised the possibility that these two proteins might form a specific complex. Results here support formation of the specific complex and provide additional evidence of interaction between Mj1338 and several other synthetases of archaeal and eukaryotic origins. Intriguingly, Mj1338 also displays an affinity for general tRNAs but not for subdomains of tRNA or microRNAs. Together, the specific affinities for synthetases and for tRNAs suggest a potential role of Mj1338 in an archaea-specific multi-synthetase complex that may involve an active collaborative networking between members of the metabolism and decoding pathways.

MATERIALS AND METHODS

Protein Expression and Purification. The gene for Mj1338 containing a C-terminal His tag was constructed in the plasmid pET22b, and mutations in the gene were created by Quik-Change site-directed mutagenesis (Strategene). Genes for the His-tagged MjProRS, human ProRS, human LysRS, and *Methanobacterium thermoautotropicum* LysRS were provided by K. Shiba (Cancer Institute). Gene expression in *Escherichia coli* BL21(DE3), cell disruption, and protein purification by the metal affinity Talon resin (ClonTech) of the cell lysate were as described previously (*23*). Affinity-purified proteins were fractionated further with the monoQ column on an FPLC system to remove contaminating nucleases. All non-His-tagged proteins were purified from the cell lysate by heat treatment (70 °C for 15 min), taking advantage of the thermostability of these proteins, and by the monoQ procedure on an FPLC system.

Mass Spectrometric Analysis. The native Mj1338 and MjProRS, copurified from the cell lysate (*21*), were loaded onto a native 8% PAGE (40 μg total). The two proteins migrated as a single band, which was excised, extracted in 300 μL of buffer [20 mM Tris-HCl (pH 7.0), 1 mM ATP, 10% glycerol, 50 mM NaCl, 10 mM β-mercaptoethanol, 1 mM EDTA, and 4 mM $MgCl_2$], and filtered (0.22 μm, Millipore Ultrafree-DA). Approximately 1% of the filtrate was applied to a Ciphergen ProteinChip containing a normal phase array and analyzed by surface-enhanced laser desorption/ionization time-of-flight (SELDI-TOF) mass spectrometry in the presence of an EAM (energy absorption matrix) solution (Ciphergen Biosystems). External standards were used for calibration.

Gel Filtration Chromatography. Recombinant protein samples (0.5 mg/200 μL of each) in the buffer [20 mM Tris-HCl (pH 8.4), 150 mM NaCl, 10 mM KPO_4, and 10 mM β-mercaptoethanol] were loaded onto a Superose 12 HR 10/30 column (Pharmacia) on an FPLC system. The column was run with a flow rate of 0.1 mL/min, and the optical density profile was monitored at 280 nm. The column was calibrated with thyroglobulin (670 kDa), bovine γ-globulin (158 kDa), chicken ovalbumin (44 kDa), equine myoglobin (17 kDa), and vitamin B_{12} (1.35 kDa), all obtained from Bio-Rad. Blue dextran 2000 (Pharmacia) was used to determine the void volume (8.0 mL).

Determination of Binding Affinity with a Bio-Sensor. The surface plasmon resonance with the BIAcore system (Uppsala, Sweden) was determined at the University of Pennsylvania (Philadelphia, PA). MjProRS, immobilized on a dextran-based chip by antibodies that recognized the His tag (Mab, Qiagen) to yield ~200 response units (RU), was used to determine the binding affinity with Mj1338. Because of the nonspecific interaction of Mj1338 with the dextran and/or the Mab antibody on the chip, a preliminary screening selected the F1 chip in the buffer of the *in vitro* pull-down assay but with 0.4% CM-dextran. Mj1338 at different concentrations was passed over ProRS at a flow rate of 10 mg/min for 2.5 min. The specific binding signal at each concentration was obtained after correction for the nonspecific signal. Parameters for association of Mj1338 and ProRS were determined using BIAcore software.

In Vitro Pull-Down Assay. Purified Mj1338 and synthetases (10 μg each) were mixed in a binding buffer [10 mM HEPES (pH 7.5), 10 mM NaCl, 1 mM $MgCl_2$, and 1 mM DTT] at 22 °C for 30 min. The mixture was incubated with an equal volume (20 μL) of the Talon resin in the same buffer with gentle shaking. The slurry was pelleted by centrifugation and washed with 200 μL of the same buffer but with 30 mM NaCl. The gel matrix was resuspended in 20 μL of the starting buffer but with 200 mM imidazole and incubated at 22 °C for 20 min to elute protein for an SDS−PAGE analysis. The DEAE fraction of *M. jannaschii* lysate was prepared as described previously (*20*), an aliquot of which (60 mg) was incubated with 1 mL of Talon previously coupled with 10 mg of His-tagged Mj1338 in the binding buffer. Unbound proteins were washed off with 30 mM NaCl in the binding buffer, while bound proteins were eluted by buffer with 0.5 M NaCl, concentrated, and assayed for aminoacylation. A control with the resin alone was performed in parallel. SDS−PAGE analysis of the bound fraction showed that 30% of the proteins are present in identical quantities in the control, indicating the amount of proteins nonspecifically bound to the resin. To correct for the nonspecifically bound proteins, aminoacylation of the bound fraction from the coupled resin (0.5 mg/mL) was compared with that of the control (30% of 0.5 mg/mL = 0.15 mg/mL).

Gel Shift Assay for tRNA Binding. T7 transcripts of ^{32}P-labeled tRNAs were purified to single species by denaturing

PAGE. A labeled tRNA was heat-denatured in TE at 75 °C for 3 min, adjusted to 1× binding buffer, spun briefly, reannealed at 37 °C for 20 min, and titrated with the recombinant Mj1338. The volume of the final binding reaction was 20 μL, and the mixture contained 4 nM tRNA (4×10^4 cpm), 25 mM sodium phosphate (pH 7.0), 75 mM KCl, 10 mM $MgCl_2$, 24% glycerol, and varying amounts of Mj1338 and was incubated at room temperature for 15 min. It was adjusted to 31% glycerol, 0.05% xylene cyanol, and 0.05% bromophenol blue, incubated at 4 °C for 15 min, and loaded on a 2% agarose gel in 0.5× TBE at 4 °C. The gel was run in 0.5× TBE at 34 V and 4 °C for 2.5 h, dried on DE81 Whatman anion exchange paper, and analyzed with a phosphorimager. The bound and free fractions of tRNA were calculated and used to determine the apparent K_d value. The tRNA concentration was determined by absorption at A_{260}, while the Mj1338 concentration was determined by the Bradford method (Bio-Rad).

RESULTS

Specific Association of Mj1338 with MjProRS. The protein Mj1338 was copurified with *M. jannaschii* ProRS (MjProRS) through four major steps of column chromatography, including DEAE, monoQ, hydroxyapatite, and blue sepharose (*21*). The copurification suggested the possibility that these two proteins might form a specific complex. To test this possibility, we examined if the two proteins would comigrate as a single (rather than two) species by native PAGE. A protein sample that contained Mj1338 and MjProRS, each in its native form as copurified from the cell lysate of *M. jannaschii* (*21*), was electrophoresed on an 8% native gel and stained with Coomassie blue. Only one band was detected (Figure 1A), which was then excised, and the protein composition of the excised band was analyzed by SDS−PAGE and shown to contain both Mj1338 and ProRS (Figure 1B). Additionally, the protein composition was also confirmed by mass spectrometry (SELDI-TOF), which revealed two major peaks (Figure 1C). The peak at 37.2 kDa corresponded to the mass of Mj1338, while the peak at 53.7 kDa corresponded to the mass of ProRS. Two other smaller peaks were also present, representing the doubly charged Mj1338 (at 18.6 kDa) and the doubly charged ProRS (at 27.1 kDa). These results confirmed that the protein sample at the end of the copurification migrated as one species on a native gel, which upon SDS−PAGE and mass spectrometry analyses was resolved to contain only Mj1338 and ProRS. This suggested that the two proteins coexisted as one protein complex that had survived the extensive purification procedure.

The formation of the Mj1338−ProRS complex was also examined by gel filtration over a calibrated FPLC Superose-12 column (Figure 1D). The recombinant Mj1338 and ProRS, alone or in combination, were tested. The protein Mj1338 alone eluted at fractions corresponding to an apparent mass of 94.7 kDa, which suggested a dimer of 38 kDa. This was separately confirmed by dynamic light scattering experiments, which determined the molecular mass of the protein as 82.8 kDa by measuring the translational diffusion coefficient (data not shown). The ProRS alone eluted at fractions corresponding to an apparent mass of 134.0 kDa, which also suggested a dimer of the 53 kDa protein and was consistent

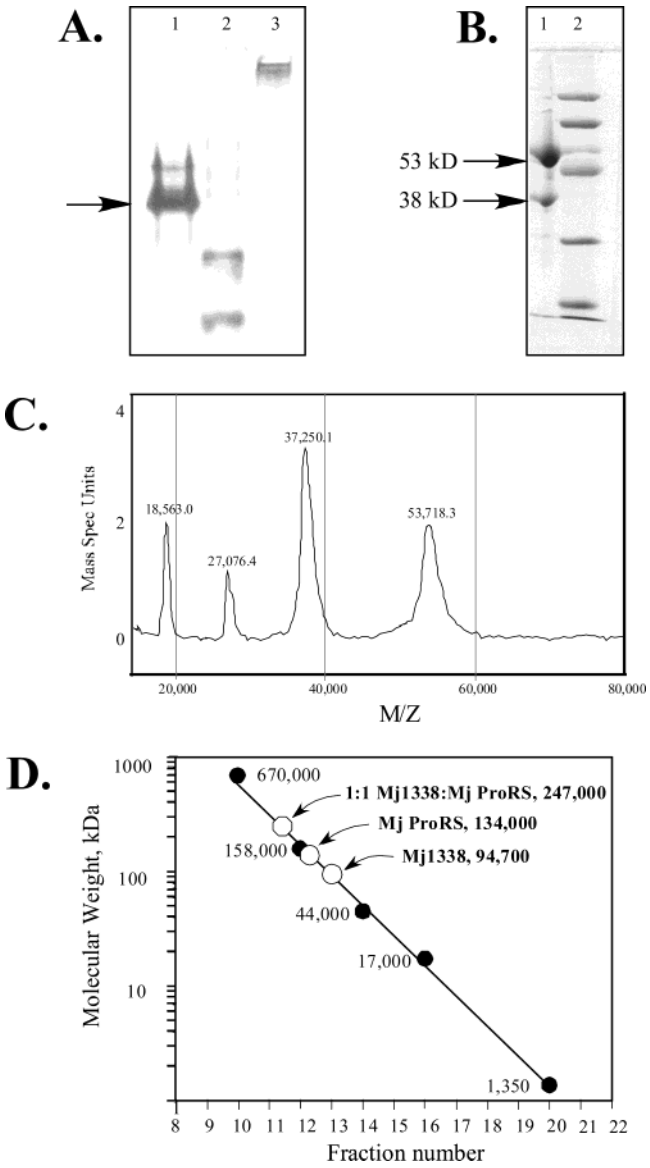

FIGURE 1: (A) Native PAGE (8%) analysis of Mj1338 and ProRS that comigrate as a single band, indicated with an arrow (lane 1). The low-molecular mass markers and BSA are shown in lanes 2 and 3, respectively. (B) SDS−PAGE (10%) analysis of the single band from panel A, showing the presence of ProRS (54 kDa) and Mj1338 (38 kDa) (lane 1) as compared to the molecular mass markers (lane 2). (C) SELDI-TOF mass spectrometric analysis of the complex of native Mj1338 and MjProRS on a Ciphergen ProteinChip. Peaks at 37.2 and 53.7 kDa are Mj1338 and ProRS, respectively, while those at 18.6 and 27.1 kDa are the doubly charged Mj1338 and ProRS, respectively. (D) Gel filtration chromatography on the Superose-12 column of the FPLC system. The elution position of Mj1338, MjProRS, and a 1:1 (molar ratio) complex of the two were overlayed with a calibration curve to yield the apparent mass of each.

with the dimeric structure observed in the crystal structure of *Tetrahymena thermophilus* ProRS (*24*). Mj1338 and MjProRS were then mixed at a 1:1 molar ratio (based on a monomer of each), and the apparent mass of the complex was determined to be 247.0 kDa, which was approximately the sum of the two individual components. Thus, the complex remained stable during chromatography, despite extensive dilution by buffer up to 50-fold. The stability suggests a specific interaction of the two proteins in a 1:1 stoichiometry.

A further test of the specific interaction between Mj1338 and ProRS was provided by surface plasmon resonance using

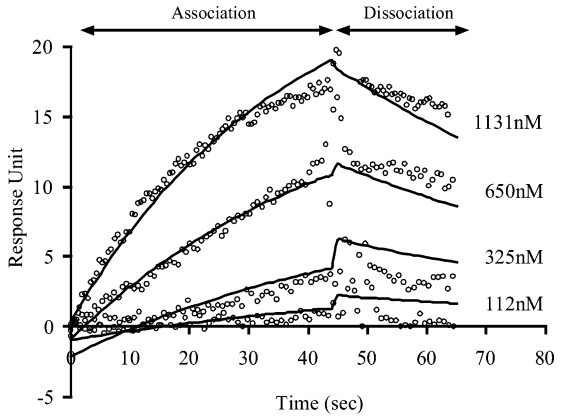

FIGURE 2: Overlay plot of the concentration-dependent binding of Mj1338 to MjProRS (His-tagged) by a BIAcore system, where the nonspecific contributions were corrected. The His-tagged ProRS (1.1 μM) was captured by a sensor chip, and buffers containing Mj1338 at the indicated concentrations were passed over the chip to assess the association between the two proteins. Subsequently, buffer alone was passed over the chip to assess the dissociation of the complex. All curves were fitted globally to a simple bimolecular model with a stoichiometry of 1:1. The time points were normalized to 100 s to compare binding and dissociation at different concentrations of Mj1338.

the BIAcore system to determine association kinetics and the equilibrium dissociation constant. The His-tagged MjProRS was immobilized to a dextran-based sensor chip through antibodies against tetra-His. A solution of increasing concentrations of Mj1338 (no tag) was passed over the immobilized ProRS to determine the kinetic parameters of the association. The reaction was carried out in 30 mM NaCl with 0.4% CM-dextran to minimize nonspecific signals. The association of Mj1338 with ProRS was monitored by the increase in response units, while the dissociation of the two was monitored upon removal of Mj1338 from the binding buffer (Figure 2). Parameters for the association and dissociation were fit to the Langmuir equation based on the 1:1 stoichiometry. The average association (k_{on}) and dissociation (k_{off}) rate constants were $(1.09 \pm 0.02) \times 10^4$ M^{-1} s^{-1} and $(1.52 \pm 0.02) \times 10^{-2}$ s^{-1}, respectively ($\chi^2 = 1.03$). These values yielded a K_d of 1.39 μM as the dissociation constant of the Mj1338−ProRS complex. Under the same conditions, binding of Mj1338 (His-tagged) with *E. coli* CysRS or with the protein ubiquitin was not observed (not shown). A similar study has been performed on the C-terminal extension peptide of human IleRS, which specifically binds the repeat units in the R domain of human Glu-ProRS. The binding interaction in this case has a K_d of 2.9 μM (*25*), similar to the K_d for the interaction between Mj1338 and ProRS.

In Vitro Pull-Down Assay of the Binding Interactions between Mj1338 and ProRS. An *in vitro* pull-down assay was developed to further test the specificity of the binding interaction between Mj1338 and ProRS. In this assay, a His-tagged protein was mixed with a protein without the tag and the mixture of the two was passed through the metal-chelated Talon resin to capture the protein that had the tag. If the two proteins were specifically bound to each other, the capture of one protein should lead to retention of the other and the complex of the two (after extensive washes) could then be eluted from the resin and examined by denaturing SDS−PAGE. Under the established assay condition, the BSA

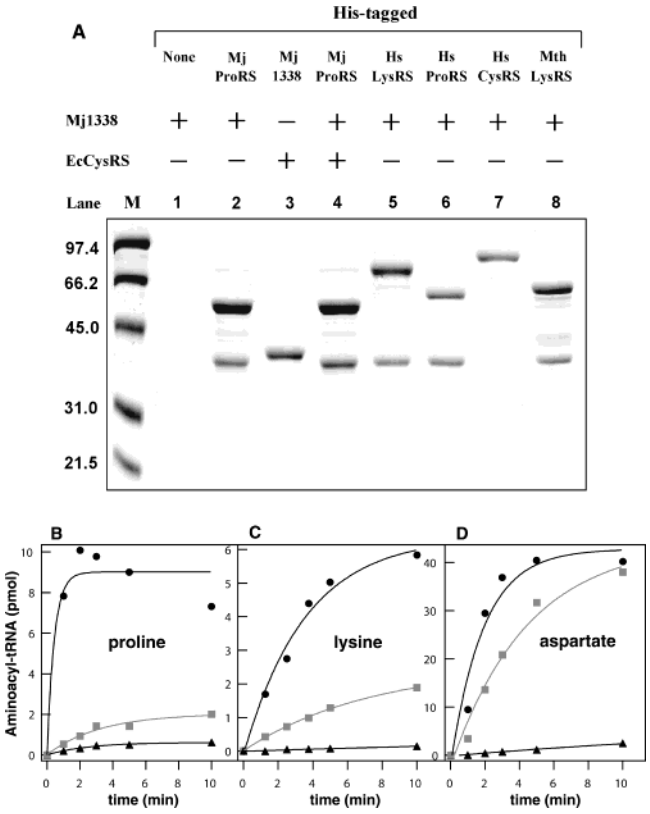

FIGURE 3: *In vitro* pull-down assay. Two protein components, one with a His tag and the other without, were mixed and subjected to Co^{2+} affinity purification *in vitro*. The proteins that were retained by the metal resin were analyzed by 10% SDS−PAGE and stained. Molecular mass markers for the gel were shown on the far left (M). Mj1338 (38 kDa), MjProRS (*M. jannaschii* ProRS, 53 kDa), EcCysRS (*E. coli* CysRS, 53 kDa), HsLysRS (*H. sapiens* LysRS, 66 kDa), HsProRS (53 kDa), HsCysRS (82.5 kDa), and MthLysRS (*Me. thermoautotropicum* LysRS, 60 kDa) were tested. Note that Mj1338 without the His tag migrated as a smaller protein (in lanes 2, 5, 6, and 8) than Mj1338 with the tag (lane 3). (B−D) Aminoacylation activities in the DEAE fraction (●), in the fraction pulled down by Mj1338 on the Talon resin (■), and in the fraction pulled down by a control resin (▲) are shown for proline (B), lysine (C), and aspartate (D).

exhibited no binding interaction with Mj1338 or any of the synthetases that were tested.

Incubation of the Talon resin with the recombinant Mj1338 without a His tag did not lead to retention of the protein (Figure 3A, lane 1), confirming that the protein alone had no affinity for the resin. However, addition to the mixture of the His-tagged MjProRS captured Mj1338 in a complex that consisted of both proteins on SDS−PAGE (53 and 38 kDa, respectively) (lane 2). This complex was retained by the resin and survived three washes before elution with imidazole. The same experiment with Mj1338 (His-tagged) and *E. coli* CysRS (no tag) only yielded the His-tagged Mj1338 (lane 3), suggesting no interaction between the two proteins. The specific association of Mj1338 with MjProRS was further confirmed by the observation that the nonspecific *E. coli* CysRS did not challenge the formation of the complex (lane 4). Additional experiments with *E. coli* AlaRS and TyrRS, and human mitochondrial LeuRS, also confirmed the lack of interaction with Mj1338 (not shown).

Association with Other Synthetases. The specific interaction of Mj1338 with MjProRS raised the question of whether Mj1338 might interact with other synthetases. Using

the *in vitro* pull-down assay, two members of the human complex, LysRS (67 kDa) and ProRS (60 kDa), were shown to form a specific complex with Mj1338 (Figure 3A, lanes 5 and 6, respectively). In contrast, human CysRS (82.5 kDa), which is not a member of the complex, did not associate with Mj1338 (lane 7). Thus, Mj1338 has specific affinities for at least two members of the human complex, and it discriminates against one synthetase not in the complex. Additionally, Mj1338 interacted with the archaea-specific LysRS of *Me. thermoautotrophicum*, which is homologous to LysRS of *M. jannaschii* and is a class I synthetase that is distinct from the class II LysRS of humans or other eukarya (*26*). This LysRS (60 kDa) formed a complex with Mj1338 (lane 8) with a specificity similar to that of Mj1338 with MjProRS and to those of Mj1338 with human LysRS and with human ProRS.

The binding interaction between Mj1338 and ProRS and LysRS was further confirmed in the cell lysate of *M. jannaschii*. This experiment was designed to identify other synthetases that might interact with Mj1338 in the cell lysate. The source of total synthetases in the cell lysate of *M. jannaschii* was prepared in a DEAE pool, which was the fraction of the lysate that was retained by the DEAE-Sepharose resin at 50 mM NaCl but eluted from the resin at 0.5 M salt. This DEAE pool, which had been confirmed previously as being highly enriched with synthetases (*20*), was passed over a Talon resin that was coupled with the His-tagged Mj1338. The resin was washed, and proteins that bound to the resin were eluted with imidazole. A parallel DEAE fraction was also passed over a control Talon resin, which was not coupled with Mj1338, to identify proteins nonspecifically bound to the resin. Aminoacylation assays determined that the ProRS and LysRS activities were both above the control levels (Figure 3B,C), indicating that both synthetases were present and retained by the resin-bound Mj1338. In addition, the AspRS activity of aminoacylation was also detected above the control (Figure 3D). Thus, at least three different synthetases (one of which is ProRS) in the DEAE fraction can associate with Mj1338. It should be noted that counterparts of all three synthetases are members of the mammalian multi-synthetase complex.

Mj1338 Recognizes General tRNA Molecules. The ability of Mj1338 to specifically bind ProRS, LysRS, and AspRS suggested the possibility of using Mj1338 as a basis to form a multi-synthetase complex similar to that of higher eukarya. Because many components of the higher eukaryotic complex have an affinity for general tRNA, we tested if Mj1338 might have the same feature. To test recognition of tRNA, we first searched for an appropriate gel shift condition. The T7 transcript of *M. jannaschii* $tRNA^{Pro}$, prepared by internal labeling, gel purified, and folded into its native structure by a heating and cooling process in the presence of $MgCl_2$, was tested with its cognate MjProRS. Many conditions were screened, ranging in gel thickness, pore size, pH, buffers, concentrations of KCl, and the voltage of electrophoresis. The one that yielded the best resolution of the bound from the free tRNA was chosen (Materials and Methods), in which the binding of $tRNA^{Pro}$ to ProRS was quantitative and easily recognizable (Figure 4A), with a K_d of 3.8 μM at 4 °C (not shown). This K_d is similar to values reported for other cognate tRNA−synthetase interactions (*5*, *27*), indicating the suitability of the assay condition. Although the $tRNA^{Pro}$−ProRS interaction should form one complex (as in Figure 4C), it occasionally appeared as two bands on the native gel (as in Figure 4A). It is possible that one band might consist of the dimer of ProRS with one molecule of $tRNA^{Pro}$, as is shown in the crystal structure of *T. thermophilus* ProRS (*24*), while the other might contain two molecules of $tRNA^{Pro}$.

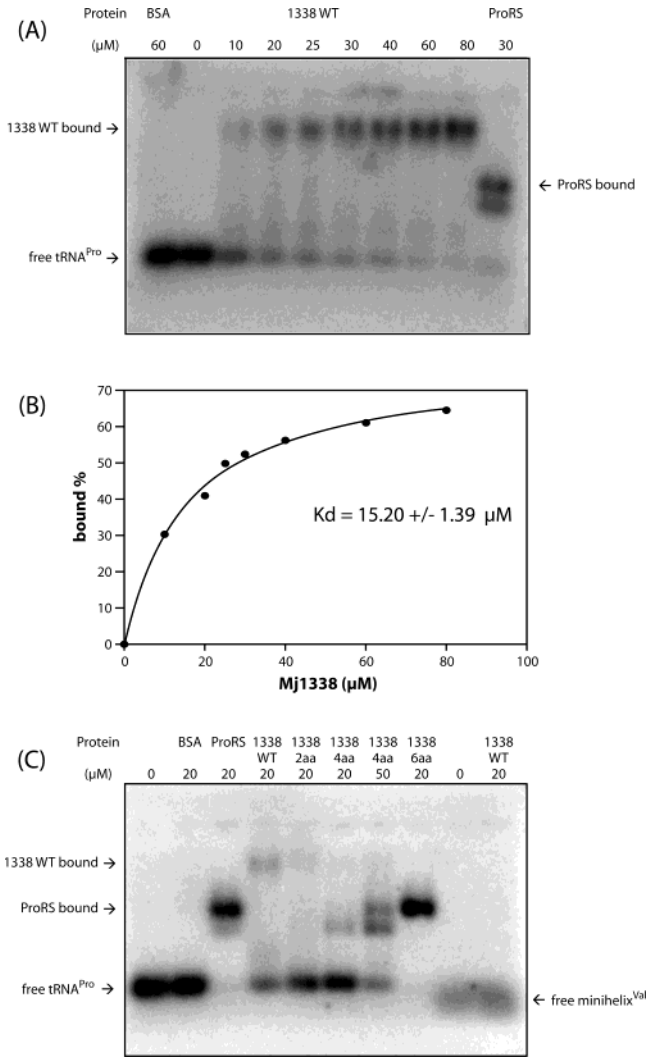

FIGURE 4: Gel shift assay of the binding interaction of *M. jannaschii* $tRNA^{Pro}$ with Mj1338. (A) The tRNA (4 nM) was incubated with Mj1338 (0−80 μM), and the shift from free to bound was visualized by a phosphorimager. BSA (60 μM) was tested as a negative control, while MjProRS (30 μM) was tested as a positive control. (B) Determination of the K_d of $tRNA^{Pro}$ for wild-type Mj1338. (C) tRNA-binding phenotype of wild-type Mj1338 and the 2aa, 4aa, and 6aa mutants at the indicated concentrations. BSA and MjProRS served as the negative and positive controls, respectively. Also, the lack of binding of the $minihelix^{Val}$ by wild-type Mj1338 is shown.

Under the identified gel shift condition, Mj1338 exhibited a binding interaction with $tRNA^{Pro}$. Specifically, titration of the protein (0−80 μM) against $tRNA^{Pro}$ (4 nM) revealed formation of a complex that appeared to be homogeneous and concentration-dependent (Figure 4A). The slower migration of the complex, compared to that of the $tRNA^{Pro}$−ProRS complex, suggested a less compact molecular shape, or a higher molecular mass consisting of multimeric Mj1338 and tRNA. Although the binding reaction was performed at 22 °C and the gel electrophoresis was at 4 °C (not the physiological temperature, 83 °C, of *M. jannaschii*), the

complex formation was specific to Mj1338 and was not detected by incubation of the tRNA with BSA at 60 μM (Figure 4A). The plot of the fraction of tRNA in the bound complex versus the concentration of Mj1338 yielded a binding curve with an apparent K_d (the concentration of Mj1338 at 50% saturation) of 15.2 μM (Figure 4B). Notably, this apparent K_d compared favorably with those of eukaryotic R domains for tRNA. For example, the K_d of the three repeats (the R3 domain) of human GluRS-ProRS for tRNA is 1−10 μM, while that of the two repeats (the R2 domain) of the hamster enzyme was 40 μM (*28*). These apparent K_d values are higher than the K_d of synthetases for their cognate tRNA, indicating a lower affinity.

The gel shift assay also detected binding of Mj1338 to transcripts of other tRNAs, such as *M. jannaschii* $tRNA^{Cys}$, $tRNA^{Ser}$, $tRNA^{Arg}$, and *E. coli* $tRNA^{Cys}$ (not shown). The binding affinity in all cases was similar to that with $tRNA^{Pro}$, indicating that Mj1338 has an affinity for general tRNA. Because the tRNAs selected for the gel shift assay differ at the N73 nucleotide prior to the CCA end, Mj1338 does not discriminate at the acceptor end. However, Mj1338 appeared to discriminate against subdomains of tRNA, because the RNA oligomer of the D-anticodon stem−loop motif of *E. coli* $tRNA^{Cys}$ (not shown), or the DNA oligomer of the minihelix of *E. coli* $tRNA^{Val}$ terminated with ribose A76 (Figure 4C), was not recognized for binding in the gel shift assay. To better determine if Mj1338 only recognizes tRNA, three other small RNAs, each with a structure different from that of the full-length tRNA, were tested. The microRNAs *lin-4* and *let-7* both regulate the timing of *Caenorhabditis elegans* development and are each complementary to the 3′ untranslated regions of a set of protein-encoding genes that are negatively regulated by the RNA (*29*, *30*). Both the *lin-4* (22-mer) and *let-7* (21-mer) RNAs can fold into a bent stem−loop secondary structure. The third RNA has a simple hairpin structure of seven base pairs in the stem and four nucleotides in the loop, flanked by single-stranded regions on the 5′ (ten nucleotides) and 3′ (four nucleotides) ends. None of the three RNAs were efficiently recognized by Mj1338, even at a concentration (40 μM) that completely shifted $tRNA^{Pro}$ (not shown). Thus, of all the RNAs that have been tested, only the full-length tRNA was recognized by Mj1338, which suggested an affinity of the protein for the tRNA L-shaped structure.

A Peptide in Mj1338 Is Similar to the Eukaryotic Repeat Units. The recognition of general tRNA indicated a functional similarity of Mj1338 to eukaryotic repeat units. A multiple-sequence alignment of several eukaryotic repeat units, particularly those found in the linker region of the bifunctional Glu-ProRS, has revealed consensus residues common to 60% of the sequences (Figure 5A) (*28*). The *Cricetulus griseus* R1b repeat (the second repeat unit in the Glu-ProRS) (*28*) and of the human R1a domain (R1, the first repeat) (*31*) have now been studied by NMR structural analysis, which has shed light on the significance of the consensus. In both structures, the repeat unit is built around an antiparallel coiled coil. Some of the consensus residues, specifically those of the aliphatic nature, are clustered to form the interior hydrophobic core, while consensus residues basic in nature are displayed on the surface and may provide the interaction with charged nucleic acids, such as tRNA (*28*, *31*). The alignment of the repeats thus provided the basis for determining if Mj1338 might harbor a similar sequence.

Table 1: Apparent K_d for tRNA Determined by the Gel Shift Assay

Mj1338	K_d (μM)	substitutions
wild-type	15.2	
mutant 1	13.2	M214A, V218A, T219A, A220G
mutant 2	22.2	V226A, L227A, Y229A
mutant 4	14.8	L252A
mutant 5	21.6	L258A, V259A, G263P
mutant 6	26.6	I264A, L271A, N272A
mutant 2aa	52.2	V248A, L252A
mutant 4aa	18.2	R234A, K235A, K241A, K242A
mutant 6aa	6.3	V248A, L252A, R234A, K235A, K241A, K242A

Using the R domains of eukaryotic Glu-ProRS as a probe, a BESTFIT (GCG) search showed that Mj1338 contains a segment of 58 amino acids (L217−E274) that is homologous. This segment shares many of the consensus residues that are predicted to be important for the function of the eukaryotic R domains (Figure 5A). For example, Mj1338 contains positively charged residues K235 and K241 and aliphatic residues V248 and L252 that are common to the consensus of the eukaryotic repeats. To test the significance of the conservation, three mutants were created and their ability to bind $tRNA^{Pro}$ was compared with that of the wild type (Figure 4C). The binding affinity of mutant 2aa, which contains the V248A and L252A substitutions, was reduced 4-fold (K_d = 52.2 μM; Table 1). Mutant 4aa, which contains the R234A, K235A, K241A, and K242A substitutions, had a mobility shift altered from that of the wild type (Figure 4C). Although the K_d of the mutant is similar to that of the wild type (K_d = 18.2 μM), the altered mobility shift suggested a change in the charge/mass ratio, which could be due to the different multimerization or molecular shape of the protein−tRNA complex. At a higher concentration of the mutant, the mobility shift changed again, suggesting that the tRNA-dependent multimerization was an important factor. Most interestingly, mutant 6aa, which combines the 2aa and 4aa mutations, had not only a mobility shift different from that of the wild type but also a 2-fold improved binding affinity (K_d = 6.3 μM). The mobility of mutant 6aa was similar to that of mutant 4aa at the higher concentration, providing additional evidence that mutations affected the multimerization state of the protein. The gel shift comparison in Figure 4C was performed with each protein at 20 μM, which is near the wild-type K_d for $tRNA^{Pro}$, so that approximately 50% of the tRNA was shifted by the wild type.

Because Mj1338 is related to the family of H_2-forming 5,10-CH_2-H_4MP dehydrogenases, which are important to the archaeal methanogens, a BLAST search was used to identify its homologues among related archaea. This search identified several homologues, among which Mj1338 aligned closely with dehydrogenase-related proteins (Figure 5B), including the ortholog Mj0715 and paralogs in *Me. thermoautotrophicum* Mth1512 and Mth504, and in *Methanocaldococcus maripaludis* Mm0782 and Mm1830. The level of overall sequence similarity with these homologues was at least 80%, with a level of identity of >60% (not shown). Mj1338 is less closely related with proteins expected to be the dehydrogenase, such as Mj0784, Mtl, Mv, Mth, or Mk. The levels of overall sequence similarity and identity with these homologues were on average greater than 50 and 30%, respectively. The alignment of the R-like motif in Mj1338

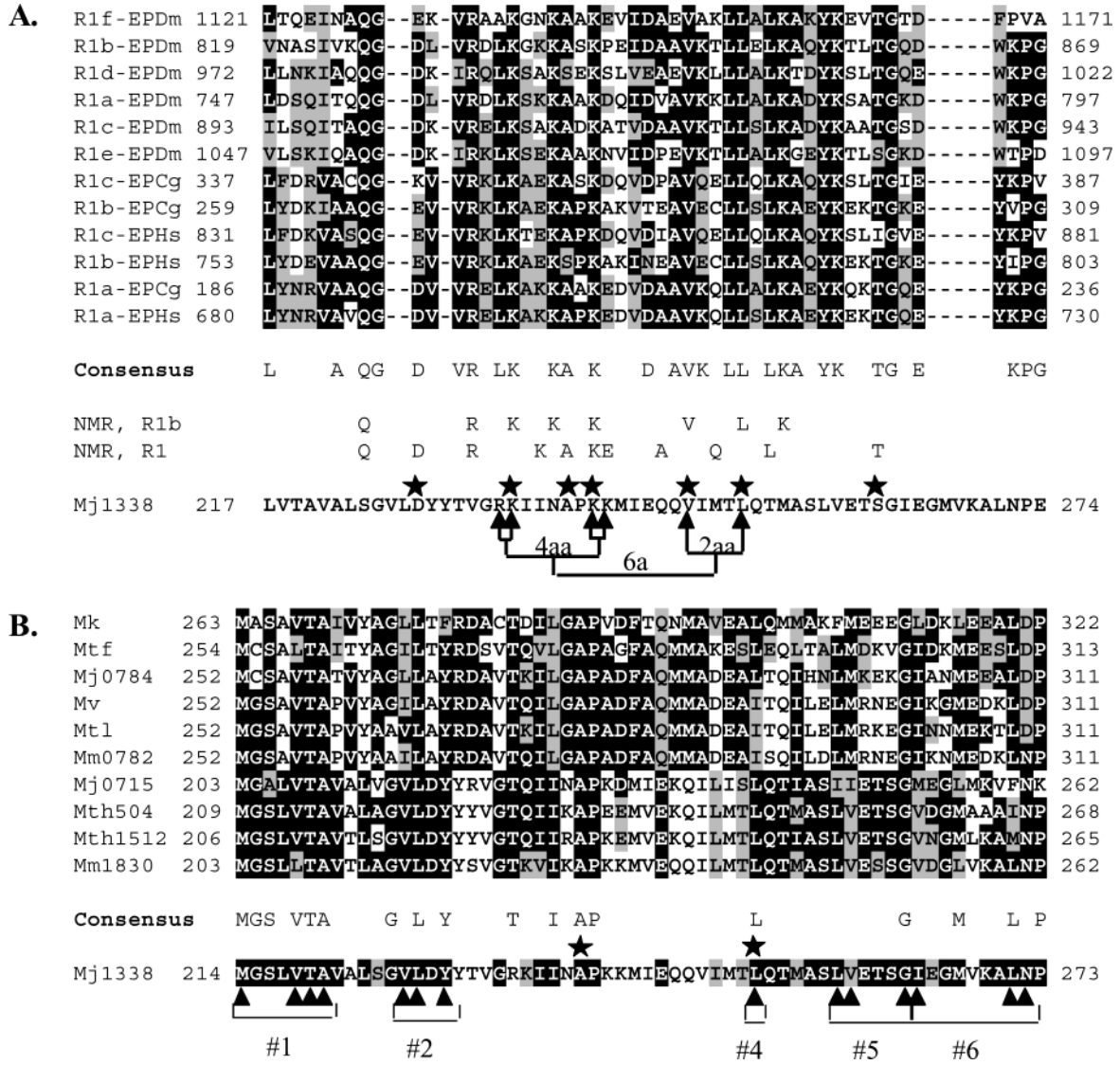

FIGURE 5: (A) CLUSTALW (*50*) alignment of eukaryotic R domains with the R domain-like region of Mj1338. The GluRS-ProRS enzyme (EP) is designated by the species [Hs (*H. sapiens*) for human, Cg (*C. griseus*) for hamster, and Dm (*D. melanogaster*) for fly]. Consensus residues (conserved in 60% of the sequences) within the R domains are highlighted in black, while residues with similar properties are in gray. Residues that are predicted to be important for RNA binding by NMR analysis of the hamster R1b (*28*) and of human R1 (*31*) are listed. Residues of Mj1338 that match these predicted functional amino acids in the consensus of the eukaryotic R domains are denoted with stars. The mutations in mutants 2aa, 4aa, and 6aa are indicated. (B) Alignment of the putative R domain of Mj1338 with archaeal homologues in *Methanopyrus kandleri* (Mk, GenBank entry Q02394), *Methanobacter thermoformicum* (Mtf, GenBank entry Q50758), *Methanocaldococcus voltae* (Mv, Q50758 Q50840), *Methanocaldococcus thermolithotrophicus* (Mtl, Q50840 Q50759), and *M. maripaludis* (Mm, 1830 and 0782). Mj and Mth (*Me. thermoautotropicum*) homologues are indicated by their open reading frame number. The alignment parameters are the same as for panel A. Residues in the consensus that are common to those of the consensus of eukaryotic R domains predicted to be important for RNA binding are denoted with stars.

with homologues of both dehydrogenase and dehydrogenase-like proteins identified 18 consensus residues (Figure 5B), although only two of these (A239 and L252) are shared with the consensus sequence of the eukaryotic repeat units. The archaeal consensus was tested in six mutants (Figure 5B), M214A, V218A, T219A, and A220G in mutant 1, V226A, L227A, and Y229A in mutant 2, L252A in mutant 4, L258A, V259A, and G263P in mutant 5, and I264A, L271A, and N272A in mutant 6. These mutations did not have an effect on tRNA binding (Table 1), in contrast to the clear effect observed for mutations in the eukaryotic consensus.

DISCUSSION

Functional Comparison of Mj1338 with Eukaryotic Repeat Units. Mj1338 is predicted to be a metabolic protein of the family of 5,10-CH_2-H_4MP dehydrogenases that catalyze the reversible dehydrogenation of methylene H_4MPT to methanyl H_4MPT and H_2. This family of H_2-forming dehydrogenases is distinct from that of the H_2-uptake dehydrogenases and is unusual in that members of the family do not mediate the reduction of one-electron acceptors (*32*). This novel class of dehydrognases, however, is widespread in methanogenic archaea. Here, the dehydrogenase activity of Mj1338 is yet to be tested, requiring development of an anaerobic assay and synthesis of the substrate methylene. Nonetheless, the close sequence homology between Mj1338 and the known H_2-forming dehydrogenases at overall levels of 50% similarity and 30% identity minimally suggests a strong possibility for the predicted metabolic function. Interestingly, Mj1338 is also functionally related to eukaryotic repeated units. The

is demonstrated in the specificity and affinity of Mj1338 in associating with several archaeal synthetases, including ProRS, LysRS, and AspRS, each of which was present in the *M. jannaschii* cell lysate (Figure 3). The strength of the binding affinities, as exemplified for the interaction between Mj1338 and ProRS (Figure 2), is quantitatively similar to those described for the eukaryotic repeats. In addition, Mj1338 recognizes general tRNA molecules, and this recognition is dependent on a motif of 58 residues that is homologous to sequences of the eukaryotic repeats. Notably, Mj1338 has two homologues in *M. jannaschii*, Mj0784 and Mj0715 (Figure 5B), which share the putative R domain and are presumably capable of binding general tRNA as well. Several homologues are also present in the genome of *Me. thermoautotropicum* and in related archaea. The multiplicity of Mj1338 in one organism is similar to the multiplicity of the eukaryotic repeats in the bifunctional GluRS-ProRS enzyme and in the mammalian multi-synthetase complex.

The general tRNA binding affinity of Mj1338, however, has features distinct from those of the eukaryotic repeats. First, of a range of nucleic acid substrates that were tested, including structured and unstructured DNA and RNA mini-helices (Figure 4), Mj1338 only recognizes the full-length tRNA substrates. In contrast, eukaryotic repeats can bind DNA, and structured and unstructured RNA molecules (*25*). The strong emphasis of Mj1338 on the full-length tRNA molecules is similar to that of TrbpIII, which is a protein of 111 amino acids from *Aquifex aeolicus* (*23*, *33*, *34*), even though the two proteins are not strongly homologous. Recent studies of TrbpIII showed that the protein specifically recognizes the outside corner of the tRNA L shape (*35*). Presumably, because *A. aeolicus* is a hyperthermophile that grows at near-boiling water temperatures, the protein TrbpIII may act as a chaperone to cover and protect tRNA. Similarly, *M. jannaschii* is a hyperthermophile, and it may depend on Mj1338 and its homologues to stabilize general tRNA. This stabilization function is not so critical for tRNA of mesophilic eukarya, and is thus not manifested in the eukaryotic repeats. It is conceivable that structure-specific tRNA binding proteins, such as TrbpIII and Mj1338, may have played a historical role in the development of the tRNA molecule.

A second feature in which Mj1338 differs from eukaryotic repeats in tRNA binding is the use of the conserved basic residues. In the NMR structures of the R1a and R1b repeats, the conserved lysines are displayed on the surface of the coiled coil and are predicted to interact with the negatively charged tRNA (*28*, *31*). This prediction is not born out by mutational analysis of Mj1338 (Figure 4C). Specifically, elimination of basic charged amino acids (R234A, K235A, K241A, and K242A) in Mj1338 changes the molecular shape of the binding (mutant 4aa), while two additional mutations of aliphatic residues (V248A and L252A) actually improve the binding (mutant 6aa). A major factor in determining the molecular shape appears to be multimer formation of the protein. Collectively, these results suggest the importance of a protein hydrophobic core such that mutations of bulky residues to alanine (V248A and L252A) that decrease hydrophobicity reduce the extent of binding (mutant 2aa), while mutations that increase hydrophobicity increase the extent of binding (mutant 6aa). Thus, Mj1338 by itself may be a weak tRNA-binding protein, but a few mutations that enhance hydrophobicity improve its tRNA affinity.

The importance of a hydrophobic core in proteins that bind nucleic acids has been widely recognized. For example, in the RMA−protein interaction within the ribosomal S8 protein−rRNA complex, the most prominent feature is the fact that the conserved side chain amino acids and bases are involved in maintaining tertiary folds. The specificity of binding is mainly driven by shape complementarity, which is increased by residues that form the hydrophobic core (*36*). In the NMR studies of the R1a and R1b repeats (*28*, *31*), the hydrophobic core contains intra- and interhelical strands that interact with each other to form the helix−turn−helix motif, which is also present in the general tRNA-binding domain of human MetRS (*8*). It is likely that the putative R domain of Mj1338 contains a hydrophobic core, which directly contributes to tRNA recognition. Alternatively, because Mj1338 is a dimer [as shown by both the gel filtration (Figure 1D) and dynamic light scattering experiments], this hydrophobic core may also stabilize the dimer interface. In the crystal structure of the tRNA-binding domain of p43, a hydrophobic core forms an interdomain interface that mimics dimer formation of general tRNA binding proteins (*37*). Clearly, to better understand the tRNA binding affinity of Mj1338, structural analysis of the putative R domain, alone and in complex with a bound tRNA, will be necessary.

A Possible Role of Mj1338 in a Multi-Synthetase Complex. It is tempting to speculate that Mj1338 and its homologues may provide the basis for forming an archaeal-specific multi-synthetase complex similar to that of higher eukarya. The copurification of Mj1338 with ProRS from the cell lysate of *M. jannaschii* suggests that these two proteins already coexist in a native complex (Figure 1), and that the complex is stable enough to have survived the extensive separation procedures. Whether other synthetases might be associated with the complex during the copurification is not known, as proteins in the intermediate stages of the purification were not analyzed. In addition, Mj1338 can associate with ProRS, LysRS, and AspRS in the cell lysate (Figure 3), indicating the possibility of forming a complex that contains at least three different synthetases. Further, Mj1338 can bind synthetases that are in the eukaryotic complex, such as ProRS and LysRS, but not CysRS. The interaction with human ProRS is similar to that with human IleRS, which is a member of the multi-synthetase complex. In a genome-wide search for interaction using the yeast two-hybrid system, the C-terminal peptide of human IleRS was found to interact with only repeats in human ProRS (*38*). The interaction of Mj1338 with human LysRS is similar to that of the p38 protein, which is the core component of the multi-synthetase complex and was found to specifically bind LysRS, Glu-ProRS, and other members of the human multi-synthetase complex in a yeast two-hybrid system (*15*). As with Mj1338, the p38 protein is also a dimer (*15*). Thus, important features that promote protein−protein interactions in the multi-synthetase complex are common between Mj1338, the repeats, and the p38 core protein.

To rigorously test the role of Mj1338 in formation of archaea-specific multi-synthetase complexes, further experiments are clearly necessary. For example, if Mj1338 is indeed the core for a multi-synthetase complex, then formation of the complex, possibly one consisting of ProRS, LysRS, and AspRS, must depend on Mj1338. This possibility can be

addressed by the *in vitro* pull-down assay, using ProRS as the anchor. In this assay, the ability of ProRS to pull down the other two synthetases should be determined by the presence of Mj1338. Second, if Mj1338 and ProRS coexist in a larger complex that includes several other synthetases, all of these synthetases should cofractionate together in the cell lysate. Thus, the fractionation procedures that were used to isolate the mammalian multi-synthetase complex (*39*−*41*) should be applied to the cell lysate of *M. jannaschii* to determine if Mj1338, ProRS, LysRS, and AspRS cofractionate in a complex larger than the size of individual proteins. Third, if the biological significance of Mj1338 in complex formation is confirmed, then the role of the putative R domain should be examined. Mutations in the R domain should be created to test the effect on complex formation. It will be also of interest to determine if the R domain-like peptide in Mj1338 by itself can associate with ProRS and with several other synthetases. All of these experiments will provide important new insights into the possibility of an archaea-specific multi-synthetase complex and the role of Mj1338 in this complex.

Evolutionary Traces of the Multi-Synthetase Complex. Lower eukaryotes lack the elaborate multi-synthetase complex of humans but contain a prototype of the complex made up of a limited number of synthetases. For example, MetRS and GluRS in yeast form a complex with the Arc1p protein, which is a *trans*-acting tRNA-binding protein that has a preferential affinity for $tRNA^{Met}$ and $tRNA^{Glu}$ (*14*). Arc1p can bring cognate partners of tRNA and synthetase together to enhance their respective aminoacylation efficiency (*42*). The tRNA-binding domain of Arc1p is homologous to the eukaryotic R domains and is also found in the p43 protein of the human complex. This domain, when examined separately from the domain that binds synthetases, displays a general affinity for RNA and can functionally substitute for a domain of yeast GlnRS that binds RNA (*42*, *43*). The association of Arc1p with two synthetases thus creates a complex that mimics a substructure of the mammalian complex.

In bacteria, although a multi-synthetase complex is not detected, trace evidence of organizing protein−protein interactions to promote general tRNA binding has been found. For example, the TrbpIII protein, which is homologous with the tRNA-binding domain of Arc1p, has general tRNA binding affinity (*23*). A TrbpIII-like domain has been identified in the C-terminus of *E. coli* MetRS (*23*), which is believed to modulate interaction of the synthetase with tRNA (*44*). Also, the N-terminus of the β-subunit of *E. coli* PheRS is homologous to TrbpIII (*14*), and is structurally similar to the OB fold (oligonucleotide/oligosaccharide binding) that binds double-stranded RNA (*45*). This domain is positioned at the entrance of the tRNA-binding cavity and may be useful for the first step of binding tRNA (*46*, *47*). The TrbpIII-like domain in MetRS and PheRS is not essential for aminoacylation (*48*), but can be viewed as the simplest substructure of the eukaryotic complex that improves tRNA binding.

Thus, evolutionary traces of organization of a multi-synthetase complex can be found from bacteria to higher eukarya. The discovery of Mj1338 and its association with ProRS has established the existence of a native protein complex that can provide the basis for forming multi-synthetase complexes in at least some branches of the archaeal domain. Clearly, additional work is necessary to explore the possibility of archaeal multi-synthetase complexes. Interestingly, unlike members of the eukaryotic complex, Mj1338 by sequence annotation is a metabolic protein. Although the metabolic activity of Mj1338 remains to be tested (*49*), Mj1338 may be a shared component that crosses the boundaries between the metabolic and decoding pathways. This would suggest an unexpected connection between metabolism and decoding, and provide an example of an archaeal enzyme that is optimized for two distinct activities in unrelated pathways that in bacteria and eukarya are typically carried out by distinct gene products. Thus, additional studies of Mj1338 will undoubtedly provide new insights into the functional genomics of archaea.

ACKNOWLEDGMENT

We thank Dr. John Leigh (University of Washington) for unpublished information on *M. maripaludis* and Dr. Gabriela Canziani (University of Pennsylvania) for the BIAcore analysis.

REFERENCES

1. Ibba, M., and Söll, D. (2000) *Annu. Rev. Biochem. 69*, 617−650.
2. Schimmel, P., Giegé, R., Moras, D., and Yokoyama, S. (1993) *Proc. Natl. Acad. Sci. U.S.A. 90*, 8763−8768.
3. Cusack, S. (1997) *Curr. Opin. Struct. Biol. 7*, 881−889.
4. Rubelj, I., Weygand-Durasevic, I., and Kucan, Z. (1990) *Eur. J. Biochem. 193*, 783−788.
5. Frugier, M., Moulinier, L., and Giege, R. (2000) *EMBO J. 19*, 2371−2380.
6. Agou, F., Waller, J. P., and Mirande, M. (1996) *J. Biol. Chem. 271*, 29295−29303.
7. Francin, M., Kaminska, M., Kerjan, P., and Mirande, M. (2002) *J. Biol. Chem. 277*, 1762−1769.
8. Kaminska, M., Shalak, V., and Mirande, M. (2001) *Biochemistry 40*, 14309−14316.
9. Norcum, M. T., and Dignam, J. D. (1999) *J. Biol. Chem. 274*, 12205−12208.
10. Mirande, M. (1991) *Prog. Nucleic Acid Res. Mol. Biol. 40*, 95−142.
11. Cerini, C., Kerjan, P., Astier, M., Gratecos, D., Mirande, M., and Semeriva, M. (1991) *EMBO J. 10*, 4267−4277.
12. Quevillon, S., Agou, F., Robinson, J. C., and Mirande, M. (1997) *J. Biol. Chem. 272*, 32573−32579.
13. Popenko, V. I., Ivanova, J. L., Cherny, N. E., Filonenko, V. V., Beresten, S. F., Wolfson, A. D., and Kisselev, L. L. (1994) *Eur. J. Cell Biol. 65*, 60−69.
14. Simos, G., Segref, A., Fasiolo, F., Hellmuth, K., Shevchenko, A., Mann, M., and Hurt, E. C. (1996) *EMBO J. 15*, 5437−5448.
15. Quevillon, S., Robinson, J. C., Berthonneau, E., Siatecka, M., and Mirande, M. (1999) *J. Mol. Biol. 285*, 183−195.
16. Quevillon, S., and Mirande, M. (1996) *FEBS Lett. 395*, 63−67.
17. Stapulionis, R., and Deutscher, M. P. (1995) *Proc. Natl. Acad. Sci. U.S.A. 92*, 7158−7161.
18. Negrutskii, B. S., and Deutscher, M. P. (1991) *Proc. Natl. Acad. Sci. U.S.A. 88*, 4991−4995.
19. Goldgur, Y., and Safro, M. (1994) *Biochem. Mol. Biol. Int. 32*, 1075−1083.
20. Hamann, C. S., Sowers, K. R., Lipman, R. S., and Hou, Y. M. (1999) *J. Bacteriol. 181*, 5880−5884.
21. Lipman, R. S., Sowers, K. R., and Hou, Y. M. (2000) *Biochemistry 39*, 7792−7798.
22. Stathopoulos, C., Li, T., Longman, R., Vothknecht, U. C., Becker, H. D., Ibba, M., and Söll, D. (2000) *Science 287*, 479−482.
23. Morales, A. J., Swairjo, M. A., and Schimmel, P. (1999) *EMBO J. 18*, 3475−3483.
24. Yaremchuk, A., Cusack, S., and Tukalo, M. (2000) *EMBO J. 19*, 4745−4758.

25. Rho, S. B., Lee, J. S., Jeong, E. J., Kim, K. S., Kim, Y. G., and Kim, S. (1998) *J. Biol. Chem. 273*, 11267−11273.
26. Ibba, M., Morgan, S., Curnow, A. W., Pridmore, D. R., Vothknecht, U. C., Gardner, W., Lin, W., Woese, C. R., and Söll, D. (1997) *Science 278*, 1119−1122.
27. Bullock, T. L., Sherlin, L. D., and Perona, J. J. (2000) *Nat. Struct. Biol. 7*, 497−504.
28. Cahuzac, B., Berthonneau, E., Birlirakis, N., Guittet, E., and Mirande, M. (2000) *EMBO J. 19*, 445−452.
29. Lee, R. C., Feinbaum, R. L., and Ambros, V. (1993) *Cell 75*, 843−854.
30. Reinhart, B. J., Slack, F. J., Basson, M., Pasquinelli, A. E., Bettinger, J. C., Rougvie, A. E., Horvitz, H. R., and Ruvkun, G. (2000) *Nature 403*, 901−906.
31. Jeong, E. J., Hwang, G. S., Kim, K. H., Kim, M. J., Kim, S., and Kim, K. S. (2000) *Biochemistry 39*, 15775−15782.
32. Zirngibl, C., Van Dongen, W., Schworer, B., Von Bunau, R., Richter, M., Klein, A., and Thauer, R. K. (1992) *Eur. J. Biochem. 208*, 511−520.
33. Swairjo, M. A., Morales, A. J., Wang, C. C., Ortiz, A. R., and Schimmel, P. (2000) *EMBO J. 19*, 6287−6298.
34. Nomanbhoy, T., Morales, A. J., Abraham, A. T., Vortler, C. S., Giege, R., and Schimmel, P. (2001) *Nat. Struct. Biol. 8*, 344−348.
35. Kushiro, T., and Schimmel, P. (2002) *Proc. Natl. Acad. Sci. U.S.A. 99*, 16631−16635.
36. Tishchenko, S., Nikulin, A., Fomenkova, N., Nevskaya, N., Nikonov, O., Dumas, P., Moine, H., Ehresmann, B., Ehresmann, C., Piendl, W., Lamzin, V., Garber, M., and Nikonov, S. (2001) *J. Mol. Biol. 311*, 311−324.
37. Renault, L., Kerjan, P., Pasqualato, S., Menetrey, J., Robinson, J. C., Kawaguchi, S., Vassylyev, D. G., Yokoyama, S., Mirande, M., and Cherfils, J. (2001) *EMBO J. 20*, 570−578.
38. Rho, S. B., Lee, K. H., Kim, J. W., Shiba, K., Jo, Y. J., and Kim, S. (1996) *Proc. Natl. Acad. Sci. U.S.A. 93*, 10128−10133.
39. Kisselev, L. L., and Wolfson, A. D. (1994) *Prog. Nucleic Acid Res. Mol. Biol. 48*, 83−142.
40. Yang, D. C. H. (1996) *Curr. Top. Cell. Regul. 34*, 101−136.
41. Nathanson, L., and Deutscher, M. P. (2000) *J. Biol. Chem. 275*, 31559−31562.
42. Simos, G., Sauer, A., Fasiolo, F., and Hurt, E. C. (1998) *Mol. Cell 1*, 235−242.
43. Whelihan, E. F., and Schimmel, P. (1997) *EMBO J. 16*, 2968−2974.
44. Valenzuela, D., and Schulman, L. H. (1986) *Biochemistry 25*, 4555−4561.
45. Murzin, A. G. (1993) *EMBO J. 12*, 861−867.
46. Mosyak, L., Reshetnikova, L., Goldgur, Y., Delarue, M., and Safro, M. G. (1995) *Nat. Struct. Biol. 2*, 537−547.
47. Goldgur, Y., Mosyak, L., Reshetnikova, L., Ankilova, V., Lavrik, O., Khodyreva, S., and Safro, M. (1997) *Structure 5*, 59−68.
48. Cassio, D., and Waller, J. P. (1971) *Eur. J. Biochem. 20*, 283−300.
49. Klein, A. R., and Thauer, R. K. (1997) *Eur. J. Biochem. 245*, 386−391.
50. Thompson, J. D., Higgins, D. G., and Gibson, T. J. (1994) *Nucleic Acids Res. 22*, 4673−4680.

BI0344533